JOC Article
pubs.acs.org/joc

Superaromatic Terpyridines: Hexa-*peri*-hexabenzocoronenes with Tridentate Functionality

Frances A. Murphy and Sylvia M. Draper*

School of Chemistry, Trinity College Dublin, D2, Ireland

smdraper@tcd.ie

Received November 27, 2009

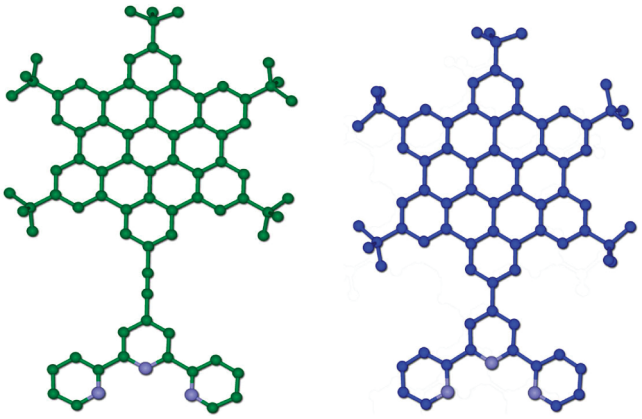

Two superaromatic terpyridine ligands (**1** and **2**) incorporating a hexa-*peri*-hexabenzocoronene (HBC) unit at the 4′-position have been prepared. In **1**, the terpyridine and the HBC domains are directly fused, while in **2**, they are separated by an acetylene linker. Also presented is the synthesis and characterization of several novel HBC derivatives, including 2-iodo-5,8,11,14,17-penta-*tert*-butyl-hexa-*peri*-hexabenzocoronene (**7**), a valuable synthetic intermediate. Different synthetic routes to **1** and **2** are employed, and two alternative methods resulted in excellent yields of **2**. The optical properties of both novel terpyridines are examined using UV−visible absorption and emission spectroscopy. The single-crystal X-ray structures of **7** and a precursor, 4-iodo-4′-*tert*-butylphenylacetylene (**5**), are discussed.

Introduction

Hexa-*peri*-hexabenzocoronene (HBC) with 13 fused benzene rings is a large polycyclic aromatic hydrocarbon and, as such, has been the focus of considerable research. Large disk-like HBC derivatives exhibit interesting electronic and optical properties resulting from their extensive electron delocalization and intrinsic chemical stability.[1] In addition, such molecules can aggregate to form columnar stacks. Analogues of graphite (itself a highly efficient organic conductor), HBC, and related compounds are expected to provide useful components in the area of molecular electronics and optoelectronics.[2,3]

The first generation of nitrogen-containing HBC derivatives (or *hetero*superbenzenes, HSBs) were synthesized as a family of pyrimidine-containing polyaromatic compounds.[4] The addition of *ortho*-nitrogen atoms provided a site for bidentate coordination to metal centers in a manner analogous to 2,2′-bipyridine.[5−7] The result was the marriage of the intriguing properties of HBC with the exciting photophysical

(1) Haley, M. M.; Tykwinski, R. R. *Carbon-Rich Compounds: From Molecules to Materials*; Wiley-VCH: Weinheim, Germany, 2006.
(2) Mativetsky, J. M.; Kastler, M.; Savage, R. C.; Gentilini, D.; Palma, M.; Pisula, W.; Müllen, K.; Samorì, P. *Adv. Funct. Mater.* **2009**, *19*, 2486–2494.
(3) Yamamoto, Y.; Fukushima, T.; Suna, Y.; Ishii, N.; Saeki, A.; Seki, S.; Tagawa, S.; Taniguchi, M.; Kawai, T.; Aida, T. *Science* **2006**, *314*, 1761–1764.
(4) Draper, S. M.; Gregg, D. J.; Madathil, R. *J. Am. Chem. Soc.* **2002**, *124*, 3486–3487.
(5) Draper, S. M.; Gregg, D. J.; Schofield, E. R.; Browne, W. R.; Duati, M.; Vos, J. G.; Passaniti, P. *J. Am. Chem. Soc.* **2004**, *126*, 8694–8701.
(6) Gregg, D. J.; Bothe, E.; Hofer, P.; Passaniti, P.; Draper, S. M. *Inorg. Chem.* **2005**, *44*, 5654–5660.
(7) Gregg, D. J.; Fitchett, C. M.; Draper, S. M. *Chem. Commun.* **2006**, 3090–3092.

Published on Web 02/19/2010 DOI: 10.1021/jo902526u

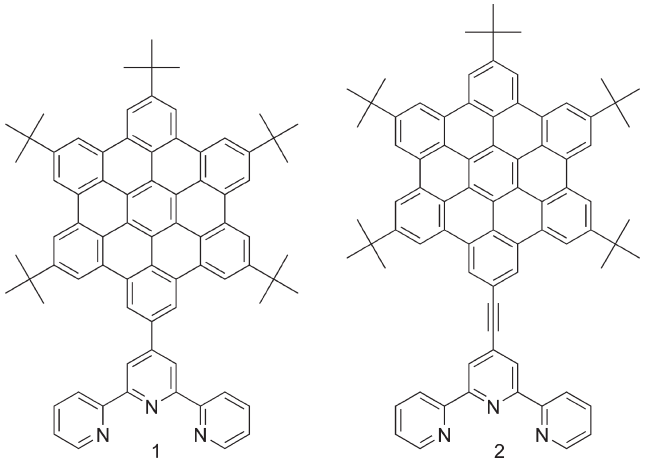

FIGURE 1. HBC−terpyridine ligands **1** and **2**.

and electrochemical properties of Ru(II) trisdiimine metal complexes. Here, in an extension to this emerging field, we present the synthesis, characterization, and photophysical study of HBC derivatives coupled to 2,2′;6′,2″-terpyridine (Figure 1). Ligand **1** consists of a terpyridine unit substituted at the 4′-position with a penta-*tert*-butyl-substituted HBC. The *tert*-butyl groups confer increased solubility to large planar molecules by reducing the propensity for aggregation in solution. Ligand **2** differs from **1** in that the terpyridine unit and the HBC platform are separated by an acetylene bridge. **1** and **2** offer direct comparison for examining the ability of the acetylene linker to promote enhanced electronic communication between the tpy and HBC units, a feature known to prolong the excited-state lifetimes in Ru(II) tpy complexes.[8] There is one example of an acetylene−HBC derivative with long-chain substituents that has been used to prepare metal complexes: a Pt(II) acetylide, which displayed intriguing photophysical properties.[9]

Terpyridine (tpy) ligands readily form coordination complexes favoring the octahedral geometry of group 8 metals such as Fe(II) and Ru(II). Bis-tpy metal complexes, unlike polypyridyl metal complexes bearing three bidentate ligands, are achiral and non-enantiomeric. The quest to design original and functional tpy ligands for metal complexation has prompted the development of a number of synthetic strategies.[10] Ligands **1** and **2** presented herein contain the largest fused aromatic substituent of any known tpy derivative. As "superaromatic" ligands, these compounds are expected to furnish metal complexes displaying optoelectronic properties arising from the extended HBC platforms and, in the case of **2**, enhanced electronic communication via the acetylene bridge. While many HBC derivatives have been prepared, there are no examples with pendant polypyridyl ligands and few studies that have focused on their important photophysical properties.

Results and Discussion

Synthesis: The syntheses of compounds **1** and **2** were different and built upon two separate synthetic strategies.

SCHEME 1. Synthesis of HBC-tpy 1, Its Uncyclized Precursor 4, and the Terpyridine-Substituted Diphenylacetylene 3[a]

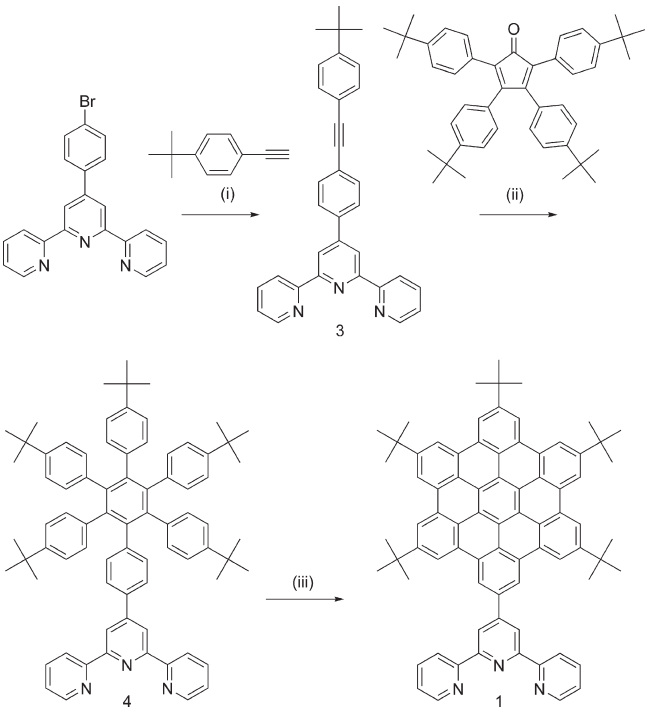

[a]Conditions: (i) triethylamine, toluene, $Pd(PPh_3)_2Cl_2$ (6 mol %), CuI (6 mol %), 70 °C, 4 h, 61%; (ii) benzophenone, 350 °C, 3.5 h, 57%; (iii) CH_2Cl_2, $FeCl_3$ (25 equiv in CH_3NO_2), 24 h, 86%.

The tpy domain was incorporated into a hexaphenylbenzene precursor, thus requiring subsequent cyclodehydrogenation in the case of **1**, while the appropriate tpy substituent was coupled to a preformed iodine-functionalized HBC unit in the case of **2**.

Taking the first strategy, the construction of the novel acetylene tpy unit, 4′-[4-(4-*tert*-butylphenyl)-ethynylphenyl]-2,2′;6′,2″-terpyridine (**3**, Scheme 1), was needed and was achieved via the coupling of 4′-(4-bromophenyl)-2,2′;6′,2″-terpyridine with 4-*tert*-butylphenylacetylene under standard Sonogashira conditions. Recrystallization of the product from hot ethanol afforded **3** in 42% yield; however, column chromatography allowed a further fraction of the product to be obtained for a total combined yield of 61%. In order to generate the hexaphenylbenzene **4**, acetylene **3** was reacted with 2,3,4,5-tetra-(4-*tert*-butylphenyl)cyclopenta-2,4-dienone via a Diels−Alder [2 + 4] cycloaddition in a benzophenone melt. **4** was isolated in 57% yield following column chromatography. Oxidative cyclodehydrogenation of **4** in methylene chloride involved the addition of excess $FeCl_3$ dissolved in nitromethane (Scheme 1(iii)). Following a short workup, column chromatography on silica gel provided **1** as a yellow solid in excellent yield. Although **1** was found to show relatively poor solubility in most common solvents, it was sufficiently soluble in $CDCl_3$ for characterization by ^1H NMR spectroscopy.

For terpyridine-substituted HBC **2**, which incorporates an acetylene bridge, a key precursor to the target compound is iodine-substituted HBC **7** (Scheme 2). The first step to iodo-HBC is the preparation of 4-iodo-4′-*tert*-butylphenylacetylene (**5**) from 4-*tert*-butylphenylacetylene and *p*-diiodobenzene under Sonogashira reaction conditions (Scheme 2(i)); **5**

(8) Hissler, M.; Harriman, A.; Khatyr, A.; Ziessel, R. *Chem.—Eur. J.* **1999**, *5*, 3366–3381.
(9) Kim, K. Y.; Liu, S.; Kose, M. E.; Schanze, K. S. *Inorg. Chem.* **2006**, *45*, 2509–2519.
(10) Schubert, U. S.; Hofmeier, H.; Newkome, G. R. *Modern Terpyridine Chemistry*; Wiley-VCH: Weinheim, Germany, 2006.

SCHEME 2. Synthesis of HBC-Actpy 2 and Its Precursors[a]

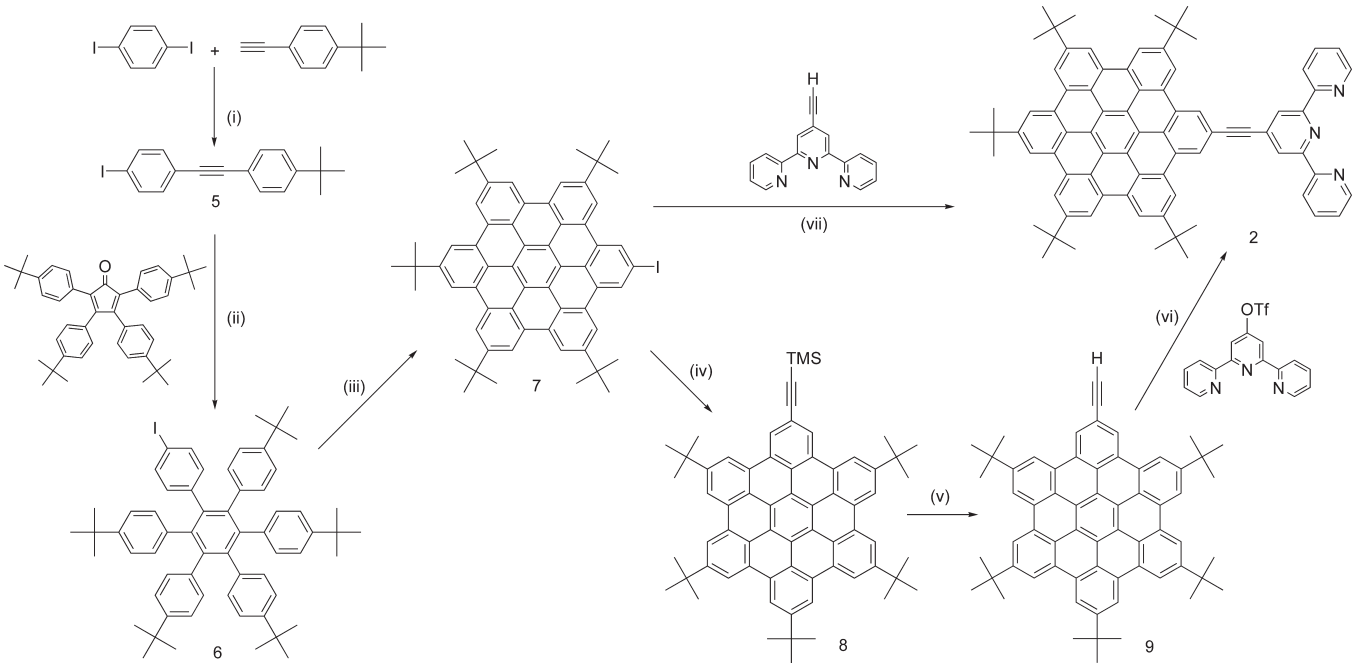

[a]Conditions: (i) diisopropylamine, THF, $Pd(PPh_3)_2Cl_2$ (5 mol %), CuI (5 mol %), 24 h, 73%; (ii) benzophenone 350 °C, 2 h, 73%; (iii) CH_2Cl_2, $FeCl_3$ (25 equiv in CH_3NO_2), 12 h, 90%; (iv) diisopropylamine, THF, $Pd(PPh_3)_2Cl_2$ (5 mol %), CuI (5 mol %), 24 h, 94%; (v) THF, methanol, KF, 12 h, 100%; (vi) toluene, diisopropylamine, $Pd(PPh_3)_4$ (5 mol %), 70 °C, 48 h, 78%; (vii) benzene, diisopropylamine, $Pd(PPh_3)_4$ (5 mol %), 70 °C, 24 h, 85%.

is obtained in 73% yield following column chromatography. **5** was then reacted with 2,3,4,5-tetra-(4-*tert*-butylphenyl)-cyclopenta-2,4-dienone via a Diels−Alder [2 + 4] cycloaddition (Scheme 2(ii)) to provide the 4-iodophenyl-substituted hexaphenylbenzene **6** in 73% yield following a chromatographic workup. The oxidative cyclodehydrogenation of **6** was then carried out to furnish iodo-HBC **7**; this was achieved by dissolving the uncyclized precursor in methylene chloride and adding an excess of $FeCl_3$ dissolved in nitromethane (Scheme 2(iii)). Addition of the reaction mixture to an excess of methanol caused the precipitation of **7** as a yellow solid.

Iodo-HBC **7**, a useful synthon for further functionalization of the HBC platform, was used to generate the target terpyridine ligand **2** via two different routes (Scheme 2). One route involves the introduction of an acetylene functional group using Sonogashira conditions to provide compound **8** and subsequently **9**. The coupling reaction (Scheme 2(iv)) proceeds smoothly at room temperature, and **8** was isolated in excellent yield after a short column. The TMS group on **8** was removed by stirring the compound in a mixture of THF and methanol overnight with KF to provide acetylene-HBC **9** in quantitative yield. **9** was reacted with triflato-tpy to afford **2** (Scheme 2(vi)). Alternatively, the direct Sonogashira coupling of **7** to 4′-ethynyl-2,2′;6′,2″-terpyridine can be employed to synthesize the same target compound (Scheme 2(vii)). Both synthetic routes to **2** are high-yielding, and since **2** is poorly soluble, it can be isolated from the reaction mixture via filtration.

NMR Spectroscopic Analysis: NMR spectroscopy was a useful tool for the characterization of the HBC compounds and their precursors. Due to the symmetry in the molecules, the ^{1}H NMR spectra of **7**, **8**, and **9** all show just six singlets in the aromatic region, while **1** and **2** have in addition a further four aromatic signals due to the terpyridine protons (see Supporting Information).

UV−Vis Absorption Spectroscopy: Absorbance spectra in THF solution were measured for iodo-HBC **7** and TMS-acetylene HBC **8** because this solvent has been reported to minimize aggregation in related compounds.[9] The spectra show features typical of other HBCs with a weak onset absorption at ca. 425 nm followed by three band maxima.[11] For **7**, these appear at 392, 361, and 345 nm, while for TMS-acetylene HBC **8**, there is a slight red shift resulting in absorptions at 394, 364, and 347 nm (Figure 2).

Although HBC-Actpy (**2**) is less soluble than the other HBC fragments presented and HBC-tpy (**1**) is soluble only in excess solvent, dilute solutions suitable for UV−visible spectroscopic measurements could be obtained. **1** dissolves completely in THF to give a clear solution at a concentration of 5×10^{-6} M. **2** dissolves slowly at the same concentration, taking up to 24 h for the solution to become completely transparent. For **1**, there are three observable maxima in the absorption spectrum that are due to the HBC chromophore, appearing at 393, 363, and 346 nm (similar to **7** and **8**). In addition, intense tpy-based $\pi-\pi^*$ and $n-\pi^*$ absorptions appear in the UV region at 243 and 228 nm (Figure 2). For **2**, the three HBC bands appear at 395, 367, and 349 nm, while the tpy-based absorptions are at 243 and 228 nm. In addition, there is a moderately intense band at 417 nm for **2**, which when observed in σ-acetylide Pt(II) complexes of dodecyl HBC was assigned to the Pt-acetylide unit.[9] A

(11) Wang, Z.; Tomovic, Z.; Kastler, M.; Pretsch, R.; Negri, F.; Enkelmann, V.; Müllen, K. *J. Am. Chem. Soc.* **2004**, *126*, 7794–7795.

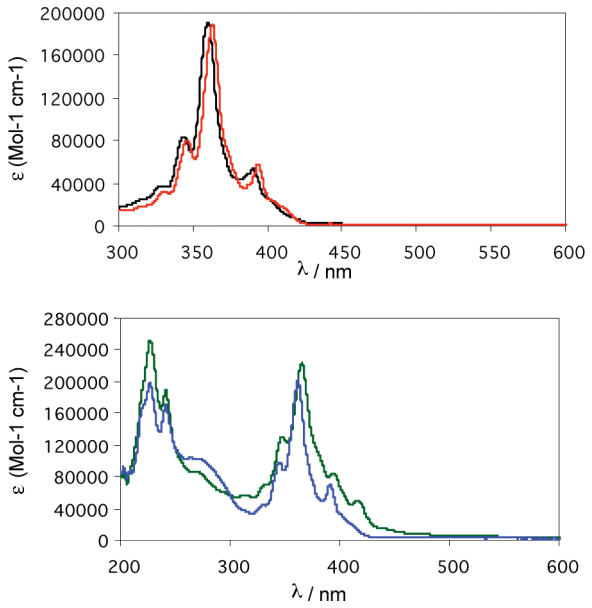

FIGURE 2. UV−vis absorption spectra of HBCs **7** (black line) and **8** (red line) and HBC-terpyridine compounds **1** (blue line) and **2** (green line) in THF (5×10^{-6} M).

similar band can be identified on the spectrum of **2** and as a shoulder in the same position for **1**.

Emission Spectroscopy: The room-temperature emission spectra of the HBC derivatives were recorded in THF at dilutions of 5×10^{-7} to 1×10^{-6} M, and both **7** and **8** were excited at the wavelength of their maximum absorption ($\lambda_{max,abs}$ = 361 nm for **7** and 364 nm for **8**). **8** emits strongly at $\lambda_{max,em}$ = 470 nm (Figure 3); however, iodo-HBC **7** is essentially nonemissive with a very weak band centered at $\lambda_{max,em}$ = 495 nm. This is expected since heavy atoms such as iodine perturb the excited-state properties of aromatic chromophores through a spin−orbital coupling mechanism (heavy atom effect).

Luminescence spectra were recorded for HBC-tpy (**1**) and HBC-Actpy (**2**) in THF at concentrations of 1×10^{-6} M. For both compounds, the spectra consist of a characteristic broad band at ~450−600 nm, having a complex vibronic structure, and resemble the emission spectrum obtained for **8**. For **1**, the most intense peak within this band occurs at 469 nm, but two overlapping peaks at 489 and 497 nm also dominate the spectrum (Figure 4). The shape and position of the emission bands remain unchanged when different excitation wavelengths are used, with the most intense emission being observed when the excitation wavelength is coincident with the maximum HBC absorption ($\lambda_{max,abs}$ = 363 nm). When the strongly absorbing tpy fragment is excited at the position of its maximum absorptions ($\lambda_{max,abs}$ = 228 and 243 nm), the luminescence detected is identical in shape and position to that observed upon irradiation at the HBC absorptions; however, the detected emission appears at much lower intensity (Figure 4).

This suggests that there is sufficient communication between the terpyridine and HBC units to allow luminescence to be observed upon excitation of the tpy unit and that the lowest emitting excited state is localized on the HBC fragment.

The luminescence spectrum obtained for HBC-Actpy (**2**) is shown in Figure 5 and also consists of a broad structured

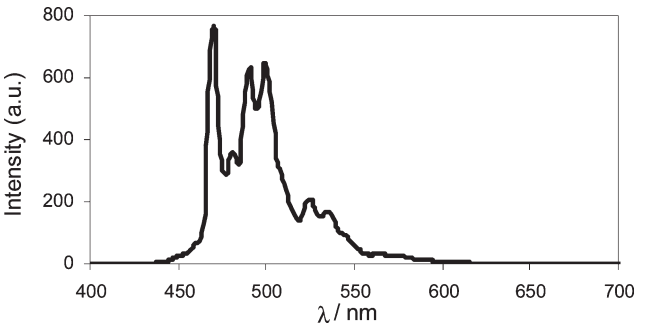

FIGURE 3. Room-temperature luminescence spectrum of **8** (5×10^{-6} M in THF).

band (~450−650 nm). The most intense peak within the emission band is observed at $\lambda_{max,em}$ = 472 nm, but the lower energy peaks at 493 and 502 nm are relatively less intense than the corresponding peaks in **1**. The emission band of **2** appears to extend toward lower energy wavelengths (> 600 nm) with a more prominent tail than that seen for **1**. The shape and position of the emission maxima remain constant when the excitation wavelength is varied, and the most intense emission appears on excitation which is coincident with the maximum HBC absorption ($\lambda_{max,abs}$ = 367 nm). When the excitation wavelength used is coincident with the intense high-energy tpy absorptions (243 and 228 nm), emission from the HBC unit is observed but at lower intensity than when the HBC unit is excited directly.

For **1** and **2**, we have established that the most intense fluorescence observed for both molecules arises from excitation at the most strongly absorbing band of the HBC platform ($\lambda_{max,abs}$ = 363 nm for **1** and 367 nm for **2**). For both compounds, the terpyridine unit absorbs strongly at 228 and 243 nm; excitation at these wavelengths also results in emission from the lowest excited state on the HBC platform. The spectra presented in Figure 4 and Figure 5 reveal that the emission observed from excitation of the tpy unit of **2** is comparatively more intense than that observed for **1**. This is summarized in Table 1, which compares the relative intensities of the λ_{max} emission peaks for **1** and **2** when the compounds are excited at their most intense HBC absorption or at the wavelengths of the tpy absorptions.

These proportionalities (Table 1) reveal information about the relative ease of energy transfer from the tpy unit to the lowest emitting excited state on the HBC unit and suggest that a more efficient transfer of energy between the two domains is possible for **2** than for **1**. This can be attributed to the presence of the acetylene bridge which facilitates electron and energy transfer between the two components, resulting in a more efficient internal conversion process in **2**.

The fluorescence quantum yields of **1** and **2** were measured in THF by comparison with a solution of the well-studied standard coumarin 153 in methanol.[12] The quantum yields were found to be approximately 0.056 and 0.071 for **1** and **2**, respectively. The excited-state lifetimes of HBC-terpyridine ligands **1** and **2** were measured at room temperature in THF at concentrations of approximately 1×10^{-6} M using a single-photon photomultiplier detection system. The excitation source used was a Hamamatsu picosecond light pulser

(12) Lewis, J. E.; Maroncelli, M. *Chem. Phys. Lett.* **1998**, *282*, 197–203.

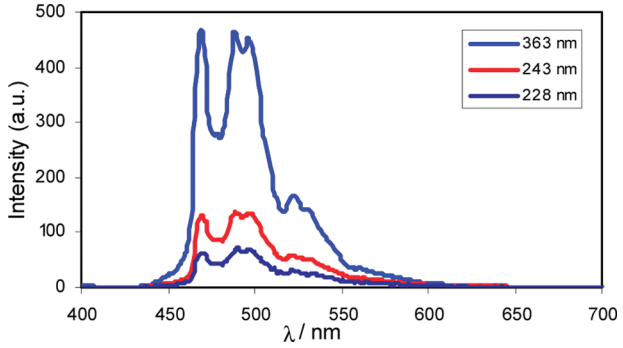

FIGURE 4. Luminescence spectra for **1** recorded at various excitation wavelengths in THF (1×10^{-6} M).

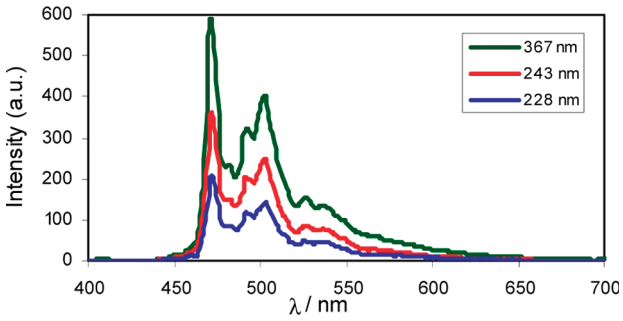

FIGURE 5. Fluorescence spectra for **2** recorded at various excitation wavelengths in THF (1×10^{-6} M).

TABLE 1. Comparative Emission Intensities for 1 and 2 at Different Excitation Wavelengths[a]

	proportion of λ_{max} HBC emission at various excitation λ		
λ_{max} emission	λ_{ex} = $\lambda_{max,abs}$ HBC[b]	λ_{ex} = 243 nm	λ_{ex} = 228 nm
1 (469 nm)	1.0	0.27	0.13
2 (472 nm)	1.0	0.61	0.35

[a]All measurements were made in argon-degassed THF solutions at 298 K. [b]The $\lambda_{max,abs}$ = 363 nm for **1** and 367 nm for **2**.

laser at 371 nm, and emission was detected at $\lambda_{max,em}$ = 469 nm for **1** and 472 nm for **2**. A decay profile of the excited state was obtained, and this was fitted to a single exponential decay model, obtaining an excellent fit for both ligands. The room-temperature excited-state lifetime for **1** was calculated to be 20.32 ± 0.03 ns. The goodness of fit between the observed decay and the single exponential model was evaluated by considering the χ^2 value, which was found to be 1.027. For **2**, the room-temperature excited-state lifetime was estimated in the same manner and was found to be 19.92 ± 0.03 ns. Clearly, the lowest excited state at room temperature on the HBC platform is relatively unaffected by the presence of the acetylene unit. A summary of the emission wavelengths, quantum yields, and fluorescence lifetimes for ligands **1** and **2** is presented in Table 2.

Crystal Structures: Crystals suitable for single-crystal X-ray diffraction were obtained for iodo-acetylene **5** and iodo-HBC **7** by slow evaporation of hexane and methylene chloride solutions, respectively. The iodo-acetylene units of **5** undergo self-assembly by close-packing with the exclusion of solvent molecules. The molecule crystallizes in a triclinic system ($P\bar{1}$) with two non-identical forms of the compound

TABLE 2. Photophysical Data for 1 and 2[a]

	emission (λ_{max}/nm)				Φ_{em}[b] (±0.01)	τ (ns) (±0.03)
1	469	489	497	522	0.056	20.32
2	472	493	502	526	0.071	19.92

[a]All measurements were made in argon-degassed THF solutions at 298 K. [b]Fluorescence quantum yields were measured relative to coumarin 153 in methanol, Φ_{em} = 0.89.[12] Measurements were made on solutions with matched optical density at 395 nm.

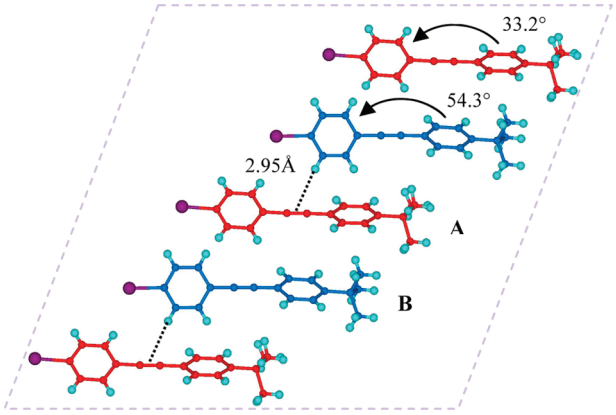

FIGURE 6. AB pairs of molecules in the crystal structure of **5**, showing the $-CH-\pi$ interaction between the iodophenyl ring in **A** and the triple bond in **B**.

(**A** and **B**) in the asymmetric unit and two **A** and **B** pairs in the unit cell. The **AB** pairs of molecules are arranged in rows of unidirectional molecules (Figure 6). In **A**, the dihedral angle between the 4-iodophenyl ring and the 4-*tert*-butylphenyl ring (33.2°) is different from that in **B** (54.3°). The acetylene triple bond length is essentially the same in both molecules (**A**, 1.202(6) Å; **B**, 1.200(6) Å). Each **AB** dimeric unit is staggered with respect to the next, with a near-linear $CH_{(\text{phenyl B unit})}-\pi_{(C\equiv C \text{ A unit})}$ interaction between adjacent **AB** units (2.95 Å and the $CH-\pi$ 171.0°) .

Both above and below the linear arrangement of dimeric units shown in Figure 6, an identical row of molecules is present orientated in the opposite direction such that the iodine substituents of the flanking rows are aligned with the *tert*-butyl groups of the first. Figure 7 shows this as viewed along the axis of the iodine substituents in Figure 6. The rows of **AB** repeating units are held together by weak interactions between adjacent molecules (e.g., $CH_{(\text{phenyl A unit})}-\pi_{(\text{phenyl B unit}}$ 2.96 Å with a $CH-\pi$ angle of 157.7°).

Iodo-HBC **7** crystallizes in the *C*2/*c* space group with one molecule in the asymmetric unit. There are eight equivalents of **7**, and no solvent molecules in the unit cell. The crystal structure shows the formation of head-to-tail dimers (Figure 8a). The benzene rings of the aromatic platforms are offset so that the center of each six-membered ring is precisely superimposed on a carbon atom in the underlying molecule. This behavior is analogous to that observed in the ideal crystal structure of graphite and is referred to as Bernal stacking;[13] it also features in the crystal structure of hexa-*tert*-butyl HBC.[14]

(13) Ebbesen, T. W. *Carbon Nanotubes: Preparation and Properties*; CRC Press: Boca Raton, FL, 1997.
(14) Herwig, P. T.; Enkelmann, V.; Schmelz, O.; Müllen, K. *Chem.—Eur. J.* **2000**, *6*, 1834–1839.

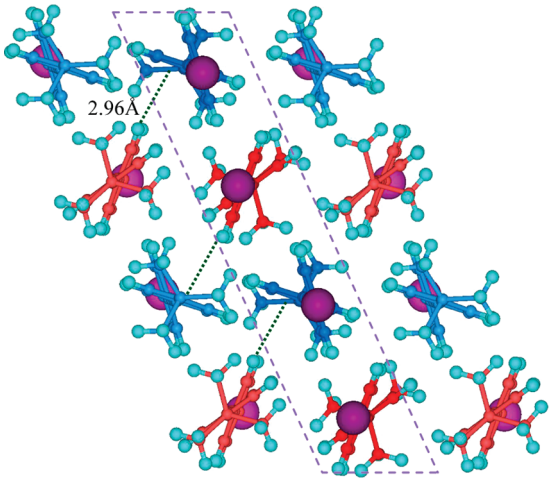

FIGURE 7. Packing of molecules in the crystal structure of **5** showing the CH−π interaction between adjacent molecules with **A** and **B** configuration.

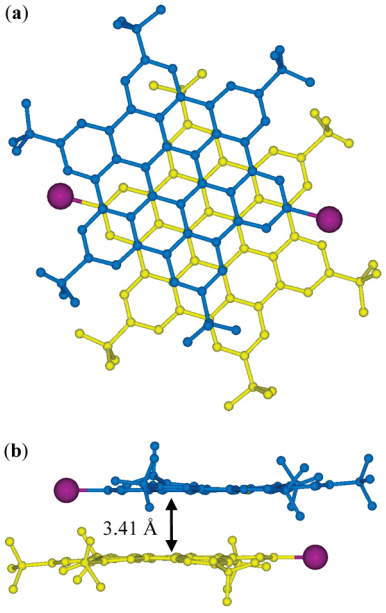

FIGURE 8. X-ray crystal structure of **7** showing the dimeric units formed (H atoms omitted for clarity). Bernal stacking as viewed from above the dimer (a) and the separation between the two molecules as viewed along the plane of **7** (b).

The interplanar distance between the iodo-HBC dimers, calculated from the aromatic core, is found to be 3.41 Å. This is remarkably close to the interplanar distance in ideal graphite (3.35 Å)[13] and closer than that observed in the crystal structure of hexa-*tert*-butyl HBC (3.44 Å). The molecules are slightly distorted from planarity at the periphery due to steric interaction between the *tert*-butyl groups of adjacent molecules (Figure 8b). The largest deviation of the central atoms on the *tert*-butyl groups from the plane calculated from the aromatic core is found to be 0.78 Å (found for the *tert*-butyl group closest to the iodine substituent which is projected over the aromatic platform of the neighboring molecule). Pairs of unidirectional dimers (and therefore rows of dimers) are offset from each other by 5.32 Å (Figure 9). The *tert*-butyl group, situated *para* to the iodine substituent, is disordered, and the partial

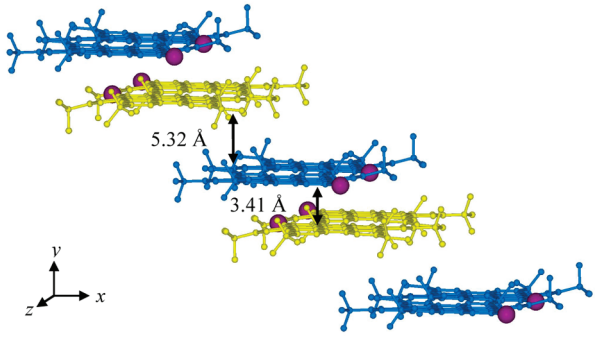

FIGURE 9. Arrangement of rows of dimers in the crystal structure of **7**.

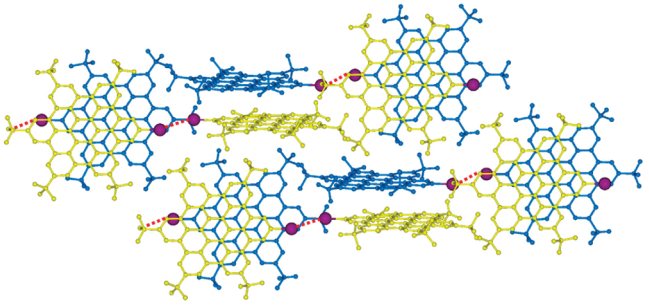

FIGURE 10. Expanded crystal packing structure of iodo-HBC (**7**) showing the I−I interactions (3.83 Å) between the dimeric units.

occupancy (80:20) was resolved by the PART command.[15] A C atom (C6) of another *tert*-butyl group exhibits a non-positive definite (even after repeated data collection at low temperature) and was refined isotropically.

Interestingly, each iodo-HBC molecule within the dimer interacts with another iodo-HBC molecule via a rarely observed iodine−iodine interaction measuring 3.83 Å (Figure 10). This compares to the sum of van der Waals radii for I−I at 3.96 Å and is relatively weak. The extended crystal structure therefore can be considered as interpenetrating rows of dimers twisted at an angle of 55.8°, whose orientation is influenced by the presence of weak iodine−iodine interactions.

Conclusion

The synthesis of a number of novel HBC derivatives and their precursors has been presented, including two unique terpyridine ligands (**1** and **2**) that contain the extended aromatic HBC core as a pendant group. Together, these compounds boast the largest fused aromatic units yet appended to a terpyridine. The synthesis of **1** required prior formation of a nonplanar hexaphenylbenzene precursor (**4**) to which oxidative cyclodehydrogenation was applied. Two alternative syntheses were presented for **2**, both requiring the synthetically useful iodo-HBC (**7**). The X-ray crystal structures of **7** and its precursor, 4-iodo-4′-*tert*-butylphenylacetylene (**5**), were obtained. The crystal structure of **7** features the replication of discrete dimers which display Bernal stacking and unusual iodine−iodine interactions. **7** readily

(15) Müller, P.; Herbst-Irmer, R.; Spek, A. L.; Schneider, T. R.; Sawaya, M. R. *Crystal Structure Refinement: A Crystallographer's Guide to SHELXL*; Oxford University Press Inc.: New York, 2006.

undergoes palladium-catalyzed Sonogashira coupling reactions, forming ligand **2** and the novel acetylene-containing HBC derivatives **8** and **9**.

All of the HBC compounds described were examined spectroscopically and displayed characteristic absorption and emission profiles. **1** and **2** were found to have excited-state lifetimes of ca. 20 ns, with **2** showing the higher quantum yield. The relative luminescence intensity detected from the HBC unit of **1** upon irradiation of the tpy absorptions was much lower than for **2**, suggesting that the acetylene bridge allows more efficient energy transfer between the two parts of the molecule.

Compounds **1** and **2** have ligand functionality and offer the exciting possibility of creating metal complexes which incorporate the properties of a graphite-like HBC chromophore. Such complexes offer intriguing opportunities for the fabrication of functional nanoscale devices and for self-assembly.[16] The preparation of a range of complexes incorporating such systems is ongoing and heralds another chapter in tpy-HBC chemistry.

Experimental Section

General Methods: 2,3,4,5-Tetra-(4-*tert*-butylphenyl)cyclopenta-2,4-dienone,[17] 4′-[{(trifluoromethyl)sulfonyl}oxy]-2,2′;6′,2″-terpyridine,[18] 4′-ethynyl-2,2′;6′,2″-terpyridine,[19] and 4′-(4-bromophenyl)-2,2′;6′,2″-terpyridine[20] were prepared following the literature procedures. All reactions were carried out under inert conditions with dry solvent, freshly distilled under anhydrous conditions. Accurate mass spectra were referenced against leucine enkephalin (555.6 g mol^{-1}) and reported within 5 ppm for electrospray mass spectra. MALDI-TOF mass spectra were recorded using an α-cyano-4-hydroxycinnamic acid matrix, and accurate mass spectra were referenced against [Glu^1]-fibrinopeptide B (1570.6 g mol^{-1}) and reported within 5 ppm. Nuclear magnetic resonance spectra were recorded in deuterated acetonitrile or chloroform with a 400 MHz spectrometer at the following frequencies: 400.13 MHz for ^{1}H and 100.6 MHz for ^{13}C or a 600 MHz spectrometer at 600.13 MHz for ^{1}H and 150.6 MHz for ^{13}C. The signals for ^{1}H and ^{13}C spectra were referenced to TMS at δ 0.0 ppm, and coupling constants were recorded in hertz (Hz) to two decimal places. All 1-D ^{1}H and ^{13}C spectra were recorded using a 400 MHz spectrometer. ^{13}C signals were assigned with the aid of DEPT 145 and DEPT 90 experiments. Two-dimensional correlation spectra were recorded on a 400 or 600 MHz spectrometer and were employed to assign the ^{1}H and ^{13}C peaks. Homonuclear correlation spectroscopy was performed using TOCSY or ^{1}H−^{1}H COSY experiments, and heteronuclear correlation spectroscopy was performed using HSQC, HMQC, or HMBC (long-range) experiments.

Photophysical Measurements: All photophysical studies were carried out with solutions contained within 1×1 cm^2 quartz cells in HPLC grade solvents and were degassed using argon bubbling. Emission quantum yields were measured in reference to coumarin 153 in methanol.[12] Excited-state lifetimes were measured using a single-photon photomultiplier detection system using a picosecond light pulser laser with a 371 nm excitation wavelength. Five thousand laser pulses were used in the experiment with a pulse width of 200 ns; the resulting data were collected, and lifetimes were determined from the observed decays. The decay was fitted using a first order exponential decay model (fit = $A + B \times e^{(-t/\tau 1)}$, where B is the pre-exponential factor and τ_1 is the lifetime of the excited state), and the goodness of fit was evaluated for each result by considering the χ^2 values and inspecting the residual plots.

X-ray Crystallography: A suitable crystal of each compound **5** and **7** was selected and mounted using inert oil on a 0.30 mm quartz fiber tip and immediately placed on the goniometer head in a 123K N_2 gas stream. The structures both converged to a reasonable R factor. Further details are provided in the Supporting Information.

4′-[4-(4-*tert*-Butylphenyl)ethynylphenyl]-2,2′;6′,2″-terpyridine (3): 4′-(4-Bromophenyl)-2,2′:6′,2″-terpyridine (250 mg, 6.44×10^{-4} mol) was dissolved in freshly distilled toluene (5 mL) and triethylamine (2 mL). CuI (7.35 mg, 3.86×10^{-5} mol) and $[Pd(PPh_3)_2Cl_2]$ (27 mg, 3.86×10^{-5} mol) were added, and the mixture was degassed. 4-*tert*-Butylphenylacetylene (0.174 mL, 9.66×10^{-4} mol) was added, and the solution was heated at 70 °C for 4 h. The brown reaction mixture was cooled, after which H_2O (50 mL) and DCM (50 mL) were added. The organic layer was separated, dried over $MgSO_4$, and evaporated to dryness. Some crystals of the product were isolated by recrystallizing from EtOH (125 mg, 42%). The remainder of the product was purified via column chromatography on silica gel, first using diethyl ether followed by a mixture of diethyl ether, MeOH, and 10% aq NH_3 (1:1:1). This provided a further 57 mg of product, total yield being 182 mg (61%): ^{1}H NMR ($CDCl_3$) δ 8.78 (m, 4 H), 8.71 (d, ^3J = 7.53 Hz, 2 H, H3), 7.93 (m, 4 H, H2a, H4), 7.69 (d, ^3J = 8.53 Hz, 2 H, H3a), 7.53 (d, ^3J = 8.03 Hz, 2 H), 7.41 (m, ^3J = 8.54 Hz, 4 H), 1.36 (s, 9 H, −CH_3 *t*-butyl); ^{13}C NMR ($CDCl_3$) δ 155.9 (2 C, quart.), 155.8 (2 C, quart.), 151.6 (1 C, quart.), 149.3 (1 C, quart.), 148.9 (2 C, −CH), 137.7 (1 C, quart.), 136.9 (2 C, −CH), 132.0 (2C, −CH), 131.3 (2C, −CH), 127.1 (2C, −CH), 125.3 (2C, −CH), 124.2 (1C, quart.), 123.8 (2C, −CH), 121.3 (2C, −CH), 119.9 (1C, quart.), 118.6 (2C, −CH), 91.0 (1C, −C≡C−), 88.3 (1C, −C≡C−), 34.7 (1C, −$C(CH_3)_3$), 31.0 (3C, −$C(CH_3)_3$); ES-MS (THF) m/z = 466.2286 $[M + H]^+$, calcd for $C_{33}H_{28}N_3$ 466.2283; IR ν (cm^{-1}) 2957 (m), 2903 (m), 2865 (m), 2217 (w), 1601 (m), 1583 (s), 1565 (s), 1541 (m), 1518 (s), 1465 (s), 1441 (m), 1409 (m), 1386 (s), 1263 (m), 1105 (m), 1075 (m), 1038 (m), 989 (m), 891 (m), 833 (s), 789 (s), 735 (s), 682 (m), 659 (s).

(1,1′-Biphenyl)-2,3,4,5,6-(4′-*tert*-butylphenyl)-4′-[2,2′:6′,2″-terpyridin]-4′-yl- (4): 3 (100 mg, 2.15×10^{-4} mol) and 2,3,4,5-tetra(4-*tert*-butylphenyl)cyclopenta-2,4-dienone (131 mg, 2.15×10^{-4} mol) were combined with 1.75 g (9.60×10^{-3} mol) of benzophenone in a 10 mL round-bottom flask. The mixture was heated on a sand microburner to 350 °C for 3.5 h under N_2 and then allowed to cool slowly to room temperature. Two milliliters of DCM was added to dissolve the reaction mixture, and this solution was added to a conical flask containing MeOH (20 mL). The mixture was heated to remove the DCM and cooled in the freezer at −10 °C to allow precipitation of an off-white solid. The solid was removed via suction filtration and washed well with MeOH (15 mL) before recrystallizing from hot MeOH to afford 106 mg (47%) of the product. The remaining mother liquor containing some product was purified via column chromatography on silica gel using ethyl acetate, increasing the gradient of triethylamine from 0 to 10% to afford a further 22 mg of the product; total yield 128 mg (57%): ^{1}H NMR ($CDCl_3$) δ 8.70 (d, ^3J = 7.53 Hz, 2 H), 8.62 (d, ^3J = 8.03 Hz, 2 H), 8.59 (s, 2 H, H3′), 7.84 (dd, ^3J = 8.03 Hz, 2 H), 7.46 (d, ^3J = 8.03 Hz, 2 H), 7.32 (dd, ^3J = 4.51 Hz, 2 H), 7.06 (d, ^3J = 8.03 Hz, 2 H), 6.86 (m, 10 H), 6.73 (m, 10 H), 1.13 (s, 45 H, −$C(CH_3)_3$); ^{13}C NMR ($CDCl_3$) δ 156.2 (quart.), 155.5 (quart.), 150.4 (quart.), 148.9 (2C, −CH), 147.8 (quart.), 147.5 (quart.), 147.4 (quart.), 142.4 (quart.), 140.8 (quart.), 140.7 (quart.),

(16) Murphy, F. A.; Suárez, S.; Figgemeier, E.; Schofield, E. R.; Draper, S. M. *Chem.—Eur. J.* **2009**, *15*, 5740–5748.
(17) Gregg, D. J.; Ollagnier, C. M. A.; Fitchett, C. M.; Draper, S. M. *Chem.—Eur. J.* **2006**, *12*, 3043–3052.
(18) Potts, K. T.; Konwar, D. *J. Org. Chem.* **1991**, *56*, 4815–4816.
(19) Grosshenny, V.; Romero, F. M.; Ziessel, R. *J. Org. Chem.* **1997**, *62*, 1491–1500.
(20) Wang, J.; Hanan, G. *Synlett* **2005**, 1251–1254.

140.2 (quart.), 139.1 (quart.), 137.9 (quart.), 137.7 (quart.), 137.0 (2 C, −CH), 134.4 (quart.), 132.2 (2 C, −CH), 131.1 (−CH phenyls), 131.1 (−CH phenyls), 125.5 (2 C, −CH), 123.8 (2 C, −CH), 123.4 (−CH phenyls), 123.11 (−CH phenyls), 123.05 (−CH phenyls), 121.3 (2 C, −CH), 118.7 (2 C, −CH), 34.14 (quart., $-C(CH_3)_3$), 34.06 (quart., $-C(CH_3)_3$), 31.2 (−CH, $-C(CH_3)_3$); ES-MS (THF) m/z = 1046.6367 $[M+H]^+$, calcd for $C_{77}H_{80}N_3$ 1046.6352; IR ν (cm^{-1}) 2960 (s), 2902 (m), 2865 (m), 1585 (m), 1567 (m), 1512 (m), 1467 (m), 1389 (s), 1361 (s), 1269 (s), 1201 (m), 1149 (m), 1118 (m), 1103 (m), 1017 (s), 859 (m), 831 (s), 793 (s), 779 (s), 738 (m), 679 (m), 661 (s).

4′-(2−5,8,11,14,17-Penta-*tert*-butylhexa-*peri*-hexabenzocoronene)-2,2′;6′,2″-terpyridine (1): 4 (40 mg, 3.82×10^{-5} mol) was dissolved in degassed DCM (50 mL) in a three-necked round-bottom flask, and nitrogen was bubbled through the solution. $FeCl_3$ (155 mg, 9.55×10^{-4} mol) was dissolved in nitromethane (2 mL) in a small Schlenk flask, and the solution was degassed. The solution was then transferred slowly into the stirring DCM solution via cannula. The resulting solution was stirred overnight with N_2 bubbling through the solution. The reaction mixture was then added to 50 mL of MeOH to obtain a red/brown solution. The solvent was removed in vacuo, and the solid obtained was purified by column chromatography on silica, first using chloroform then a mixture of $CHCl_3$/MeOH (1:1) to remove a red band due to an iron complex ($[Fe(HBC\text{-}tpy)_2](Cl)_2$). Finally, a mixture of $CHCl_3/NEt_3$ (4:1) was used to remove a yellow compound slowly from the column. The fractions containing the yellow compound were combined, and the solvent was removed to give 34 mg (86%) of the product: ^{1}H NMR ($CDCl_3$, 600 MHz) δ 9.57 (s, 2 H), 9.40 (s, 2 H), 9.36 (m, 8 H), 9.19 (s, 2 H), 8.84 (d, 2 H), 8.81 (d, 2 H), 7.96 (dd, 2 H), 7.44 (dd, 2 H), 1.87 (s, 27 H, $-C(CH_3)_3$), 1.85 (s, 18 H, $-C(CH_3)_3$); ^{13}C NMR ($CDCl_3$) δ 155.9 (quart.), 152.2 (quart.), 151.5 (quart.), 149.4 (quart.), 149.2 (quart.), 149.11 (2 C, −CH), 148.8 (quart.), 137.1 (2 C, −CH), 135.8 (quart.), 131.4 (quart.), 130.7 (quart.), 130.5 (quart.), 130.5 (quart.), 130.2 (quart.), 126.1 (quart.), 125.5 (quart.), 124.0 (quart.), 123.9 (2 C, −CH), 121.7 (2 C, −CH), 121.0 (2 C, −CH), 120.9 (quart.), 120.6 (quart.), 120.5 (2 C, −CH), 119.5 (2 C, −CH), 119.4 (2 C, −CH), 119.0 (6 C, −CH), 35.8 (quart., $-C(CH_3)_3$), 35.8 (quart., $-C(CH_3)_3$), 32.1 (−CH, $-C(CH_3)_3$), 32.0 (−CH, $-C(CH_3)_3$); MALDI-TOF MS m/z = 1033.5287, calcd for $C_{77}H_{67}N_3$ 1033.5335; IR ν (cm^{-1}) 2952 (s), 2903 (m), 2865 (m), 1604 (m), 1581 (s), (1556 (m), 1463 (m), 1392 (m), 1365 (s), 1308 (w), 1259 (s), 1200 (m), 1077 (s, br), 1016 (s, br), 940 (m), 862 (s), 787 (s), 744 (s), 728 (s), 659 (s).

4-Iodo-4′-*tert*-butylphenylacetylene (5): 4-*tert*-Butylphenylacetylene (1.37 mL, 7.58×10^{-3} mol) was dissolved in THF (20 mL). This solution was transferred via cannula to a solution of *p*-diiodobenzene (6.26 g, 1.90×10^{-2} mol), $PdCl_2(PPh_3)_2$ (27 mg, 3.8×10^{-4} mol), and CuI (7 mg, 3.68×10^{-5} mol) in diisopropylamine (15 mL) and THF (60 mL) in a Schlenk flask. The mixture was stirred overnight at room temperature under Ar. H_2O (40 mL) and DCM (100 mL) were added to the reaction mixture, and the organic layer was separated. The aqueous layer was washed with DCM (2 × 40 mL), and the combined organic fractions were dried over $MgSO_4$ and reduced in volume. The product was isolated by column chromatography (silica, hexane) resulting in 1.98 g (73%). Crystals of **5** suitable for X-ray diffraction were obtained by slow evaporation of a hexane solution: ^{1}H NMR ($CDCl_3$) δ 7.70 (d, ^3J = 8.35 Hz, 2 H), 7.48 (d, ^3J = 8.54 Hz, 2 H), 7.39 (d, ^3J = 8.54 Hz, 2 H), 7.27 (d, ^3J = 8.53 Hz, 2 H), 1.35 (s, $-C(CH_3)_3$, 9 H); ^{13}C NMR ($CDCl_3$) δ 151.4 (quart.), 137.0 (2 C, −*C*H), 132.6 (2 C, −*C*H), 130.9 (2 C, −*C*H), 125.0 (2 C, −CH), 122.6 (quart.), 119.4 (quart.), 93.4 (quart.), 90.5 (quart.), 87.4 (quart.), 34.4 (1 C (quart.), −C−$(CH_3)_3$, 30.7 (3 C, $-(CH_3)_3$); IR ν (cm^{-1}) 2952 (m), 2861 (m), 2218 (w), 1504 (m), 1478 (m), 1388 (m), 1361 (m), 1102 (m), 1002 (s), 832 (s), 819 (s), 733 (m). Anal. Calc for $C_{18}H_{17}I$: C, 60.01; H, 4.88. Found: C, 60.16; H, 4.88.

1-(4-Iodophenyl)-2,3,4,5,6-penta-(4-*tert*-butylphenyl)benzene (6): 5 (255 mg, 7.08×10^{-4} mol) and 2,3,4,5-tetra(4-*tert*-butylphenyl)cyclopenta-2,4-dienone (431 mg, 7.08×10^{-4} mol) were mixed together with benzophenone (4 g, 2.20×10^{-2} mol) in a 25 mL round-bottom flask fitted with an air condenser. The reagents were stirred together under Ar on a sand microburner at 350 °C for 2 h. The reaction mixture was cooled to room temperature and was purified by column chromatography on silica using a mixture of hexane/DCM (4:1) to give 488 mg (73%) of product: ^{1}H NMR ($CDCl_3$) δ 7.18 (d, ^3J = 8.54 Hz, 2 H), 6.87 (d, 4 H), 6.82 (m, 6 H), 6.69 (d, 6 H), 6.66 (d, ^3J = 8.53 Hz, 4 H), 6.60 (d, ^3J = 8.53 Hz, 2 H), 1.16 (s, 18 H, $-C(CH_3)_3$), 1.12 (s, 27 H, $-C(CH_3)_3$); ^{13}C NMR ($CDCl_3$) δ 147.4 (quart.), 147.0 (quart.), 147.0 (quart.), 140.4 (quart.), 140.34 (quart.), 140.26 (quart.), 139.6 (quart.), 138.1 (quart.), 137.3 (quart.), 137.2 (quart.), 137.1 (quart.), 135.0 (2 C, −CH), 133.1 (2 C, −CH), 130.6 (4 C, −CH), 130.5 (6 C, −CH), 122.9 (4 C, −CH), 122.6 (6 C, CH), 90.2 (quart.), 33.6 (5 C, quart., $-C(CH_3)_3$), 30.7 (15 C, $C(CH_3)_3$); MALDI-TOF MS m/z = 940.4470, calcd for $C_{62}H_{69}I$ 940.4444; IR ν (cm^{-1}) 2961 (s), 2903 (m), 2865 (m), 1513 (m), 1475 (m), 1148 (m), 1117 (m), 1104 (m), 1017 (m), 1009 (m), 860 (m), 829 (s), 777 (m), 680 (s). Anal. Calcd for $C_{62}H_{69}I$: C, 79.13; H, 7.39. Found: C, 78.01; H, 7.31.

2-Iodo-5,8,11,14,17-penta-*tert*-butylhexa-*peri*-hexabenzocoronene (7): 6 (250 mg, 2.66×10^{-4} mol) was dissolved in degassed DCM (100 mL) in a three-necked round-bottom flask, and a stream of N_2 was bubbled through the solution. $FeCl_3$ (862 mg, 5.13×10^{-3} mol) was quickly transferred into a Schlenk flask and dissolved in freshly distilled nitromethane (5 mL). The $FeCl_3$ solution was degassed and added slowly to the reaction flask via cannula. The reaction was stirred for 12 h with N_2 bubbling through the solution. MeOH (150 mL) was added to quench the reaction and produce a dark yellow precipitate. The yellow precipitate was filtered over Celite, washed well with MeOH, dried, and redissolved in the minimum volume of DCM. The DCM solution was passed through a short plug of silica gel to remove Fe impurities. The resulting solution was evaporated to dryness to produce **7** as an orange solid (221 mg, 90%): ^{1}H NMR ($CDCl_3$) δ 9.17 (s, 2 H), 9.09 (s, 2 H), 9.00 (s, 2 H), 8.85 (s, 2 H), 8.67 (s, 2 H), 8.55 (s, 2 H), 2.00 (s, 9 H, $-C(CH_3)_3$), 1.95 (s, 18 H, $-C(CH_3)_3$), 1.83 (s, 18 H, $-C(CH_3)_3$); ^{13}C NMR ($CDCl_3$) δ 148.1 (quart.), 147.9 (quart.), 147.8 (quart.), 131.5 (quart.), 130.0 (quart.), 129.6 (quart.), 129.3 (quart.), 129.2 (2 C, −CH), 128.0 (quart.), 123.5 (quart.), 123.0 (quart.), 122.9 (quart.), 122.7 (quart.), 119.8 (quart.), 119.4 (quart.), 119.3 (quart.), 118.7 (2 C, −CH), 118.42 (4 C, −CH), 118.35 (2 C, −CH), 118.2 (2 C, −CH), 35.7 (1 C, quart., $-C(CH_3)_3$), 35.6 (2 C, quart., $-C(CH_3)_3$), 35.5 (2 C, quart., $-C(CH_3)_3$), 32.14 (3 C, $C(CH_3)_3$), 32.09 (6 C, $-C(CH_3)_3$), 32.0 (6 C, $-C(CH_3)_3$); MALDI-TOF MS m/z = 928.3538, calcd for $C_{62}H_{57}I$ 928.3505; IR ν (cm^{-1}) 2953 (s), 2903 (m), 2865 (m), 1608 (m), 1570 (m), 1477 (m), 1460 (m), 1368 (s), 1261 (s), 1224 (m), 1201 (m), 866 (s), 850 (s), 744 (s). Anal. Calcd for $C_{62}H_{57}I$: C, 80.16; H, 6.18. Found: C, 79.04; H, 6.05.

2-Trimethylsilylethynyl-5,8,11,14,17-penta-*tert*-butylhexa-*peri*-hexabenzocoronene (8): 7 (160 mg, 1.72×10^{-4} mol), $[Pd(PPh_3)_2Cl_2]$ (7.24 mg, 1.03×10^{-5} mol), and CuI (1.97 mg, 1.03×10^{-5} mol) were dissolved in THF (15 mL) and diisopropylamine (6 mL), and the resulting solution was degassed. Trimethylsilylacetylene (0.049 mL, 3.44×10^{-4} mol) was added, and the solution was stirred overnight under N_2. The solvent was removed, and the residue was purified via column chromatography on silica using a mixture of petroleum ether/DCM (3:1) to give **8** as a bright orange solid (134 mg, 94%): ^{1}H NMR ($CDCl_3$) δ 9.10 (s, 2 H), 9.02 (s, 2 H), 8.95 (s, 2 H), 8.78 (s, 2 H), 8.60 (s, 2 H), 8.46 (s, 2 H), 2.03 (s, 9 H, $-C(CH_3)_3$), 1.98 (s, 18 H,

$-C(CH_3)_3$), 1.88 (s, 18 H, $-C(CH_3)_3$), 0.68 (s, 9 H, $-(CH_3)_3$ TMS); ^{13}C NMR ($CDCl_3$) δ 147.4 (quart.), 147.2 (quart.), 147.1 (quart.), 129.5 (quart.), 129.2 (quart.), 129.1 (quart.), 128.9 (quart.), 128.7 (quart.), 128.3 (quart.), 123.9 (2 C, −CH), 122.5 (quart.), 122.4 (quart.), 122.1 (quart.), 119.2 (quart.), 119.1 (quart.), 118.8 (quart.), 118.6 (2 C, −CH), 118.0 (2 C, −CH), 117.9 (2 C, −CH), 117.7 (2 C, −CH), 117.6 (2 C, −CH), 107.0 (1 C, −C≡C−), 94.1 (1 C, −C≡C−), 35.4 (1 C, quart., $-C(CH_3)_3$), 35.3 (2 C, quart., $-C(CH_3)_3$), 35.2 (2 C, quart., $-C(CH_3)_3$), 31.9 (3 C, $-C(CH_3)_3$), 31.84 (6 C, $-C(CH_3)_3$), 31.82 (6 C, $-C(CH_3)_3$), 0.1 (3 C, TMS); IR ν (cm^{-1}) 2953 (s), 2903 (m), 2866 (m), 2146 (m), 1607 (m), 1578 (m), 1478 (m), 1369 (m), 1362 (m), 1247 (m), 1090 (m, br), 1020 (m, br), 987 (m), 942 (m), 865 (s), 854 (s), 840 (s), 668 (s); MALDI-TOF MS m/z = 898.4916, calcd for $C_{67}H_{66}Si$ 898.4943. Anal. Calcd for $C_{67}H_{66}Si$: C, 89.48; H, 7.40. Found: C, 88.30; H, 7.33.

2-Ethynyl-5,8,11,14,17-penta-*tert*-butylhexa-*peri*-hexabenzocoronene (9): 8 (25 mg, 2.78×10^{-5} mol) was dissolved in THF (5 mL) and MeOH (5 mL). KF (5 mg, 8.61×10^{-5} mol) was added, and the mixture was stirred at room temperature for 20 h. DCM (10 mL) and H_2O (10 mL) were added to the reaction mixture, and the yellow organic phase was separated. The organic layer was dried over $MgSO_4$, and the solvent was removed in vacuo to give **9** (23 mg, 100%): ^1H NMR ($CDCl_3$) δ 9.18 (s, 2 H), 9.11 (s, 2 H), 9.03 (s, 2 H), 8.88 (s, 2 H), 8.69 (s, 2 H), 8.60 (s, 2 H), 3.63 (s, 1 H, −C≡CH), 1.98 (s, 9 H, $-C(CH_3)_3$), 1.93 (s, 18 H, $-C(CH_3)_3$), 1.83 (s, 18 H, $-C(CH_3)_3$); ^{13}C NMR ($CDCl_3$) δ 148.3 (quart.), 148.1 (quart.), 148.0 (quart.), 130.2 (quart.), 129.84 (quart.), 129.80 (quart.), 129.7 (quart.), 129.5 (quart.), 128.7 (quart.), 124.4 (2 C, CH), 123.2 (quart.), 123.1 (quart.), 122.9 (quart.), 120.1 (quart.), 119.9 (quart.), 119.6 (quart.), 119.04 (2 C, −CH), 118.97 (quart.), 118.6 (2 C, −CH), 118.5 (2 C, −CH), 118.4 (4 C, −CH), 85.9 (1 C, −C≡CH), 77.2 (1 C, −C≡CH), 35.8 (1 C, quart., $-C(CH_3)_3$), 35.7 (2 C, quart., $-C(CH_3)_3$), 35.6 (2 C, quart, $-C(CH_3)_3$), 32.2 (3 C, $-C(CH_3)_3$), 32.2 (6 C, $-C(CH_3)_3$), 32.1 (6 C, $-C(CH_3)_3$); MALDI-TOF MS m/z = 826.4547, calcd for $C_{64}H_{58}$ 826.4539; IR ν (cm^{-1}) 3310 (w), 2953 (s), 2905 (m), 2866 (m), 2163 (w), 1607 (m), 1578 (m), 1478 (m), 1459 (m), 1362 (s), 1244 (m), 1201 (m), 1503 (m, br), 1021 (m, br), 942 (m), 865 (s), 811 (s).

4′-(2-Ethynyl-5,8,11,14,17-penta-*tert*-butylhexa-*peri*-hexabenzocoronene)-2,2′;6′,2″-terpyridine (2): Route A: **7** (50 mg, 5.38×10^{-5} mol) and 4′-ethynyl-2,2′;6′,2″-terpyridine (13.9 mg, 5.38×10^{-5} mol) were dissolved in benzene (12 mL) and diisopropylamine (3 mL), and the resulting solution was degassed via three freeze−pump−thaw cycles. $Pd(PPh_3)_4$ (3.1 mg, 2.69×10^{-6} mol) was then added, and the clear yellow solution was heated to 70 °C under Ar overnight. The resulting bright yellow precipitate was cooled, and the volume of the solvent was reduced in vacuo. The insoluble yellow precipitate was removed via filtration, washed with ether, and dried (48 mg 85%). Route B: **9** (50 mg, 6.04×10^{-5} mol) and 4′-[{(trifluoromethyl)-sulfonyl}oxy]-2,2′;6′,2″-terpyridine (23 mg, 6.04×10^{-5} mol) were dissolved in toluene (15 mL) and diisopropylamine (5 mL), and the resulting solution was degassed via three freeze−pump−thaw cycles. $Pd(PPh_3)_4$ (3.5 mg, 3.23×10^{-6} mol) was then added, and the clear yellow solution was heated to 70 °C under Ar for 48 h. The reaction mixture was cooled, and the volume of solvent was reduced in vacuo. The insoluble yellow precipitate was removed via filtration, washed with ether, and dried (49.6 mg, 78%): ^1H NMR ($CDCl_3$, poorly soluble) δ 9.43 (s, 2 H), 9.35 (m, 8 H), 9.33 (s, 2 H), 8.85 (s, 2 H), 8.82 (d, 2 H), 8.66 (d, 2 H), 7.91 (dd, 2 H), 7.42 (dd, 2 H), 1.91 (s, 18 H, $-C(CH_3)_3$), 1.87 (s, 27 H, $-C(CH_3)_3$); MALDI-TOF MS m/z = 1057.5345, calcd for $C_{79}H_{67}N_3$ 1057.5335; IR ν (cm^{-1}) 2952 (s), 2903 (m), 2866 (m), 2218 (w), 1604 (m), 1581 (s), 1565 (m), 1465 (m), 1446 (m), 1391 (s), 1360 (s), 1307 (w), 1258 (s), 1200 (m), 1148 (m), 1097 (m), 999 (m), 940 (m), 882 (m), 866 (s), 810 (m), 787 (s), 764 (m), 741 (s), 672 (s), 660 (s).

Acknowledgment. The authors thank Dr. John O'Brien, Dr. Manuel Reuther, and Dr. Martin Feeney for technical assistance, and Dr. Thomas McCabe and Dr. Sunil Varughese for the X-ray crystallography. The work presented was supported financially by Science Foundation Ireland (05PICAI819) and IRCSET (PG-Murphy).

Supporting Information Available: ^1H and ^{13}C NMR spectra for compounds **1**−**9**, X-ray crystallographic information for compounds **5** and **7**. This material is available free of charge via the Internet at http://pubs.acs.org.